



# 3D graphene aerogel based photocatalysts: Synthesized, properties, and applications

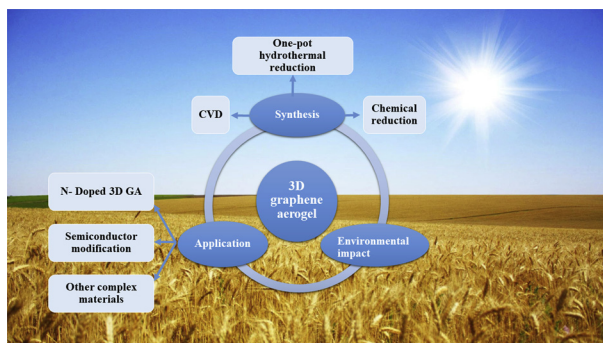


Shixia Long<sup>a,b,1</sup>, Han Wang<sup>a,b,1</sup>, Kai He<sup>a,b,1</sup>, Chengyun Zhou<sup>a,b,1</sup>, Guangming Zeng<sup>a,b,\*</sup>, Yue Lu<sup>a,b,\*</sup>, Min Cheng<sup>a,b</sup>, Biao Song<sup>a,b</sup>, Yang Yang<sup>a,b</sup>, Ziwei Wang<sup>a,b</sup>, Xiaozhe Luo<sup>a,b</sup>, Qingqing Xie<sup>a,b</sup>

<sup>a</sup> College of Environmental Science and Engineering, Hunan University, Changsha, 410082, China

<sup>b</sup> Key Laboratory of Environment Biology and Pollution Control, Hunan University, Ministry of Education, Changsha, 410082, China

## GRAPHICAL ABSTRACT



## ARTICLE INFO

### Keywords:

Three-dimensional graphene aerogel  
Organic dyes  
Photocatalysis  
Degradation

## ABSTRACT

Photocatalysis has been regarded as one of the promising approaches to solve environmental problems. Three-dimensional graphene aerogel (3D GA) is a novel photocatalytic material with unique porous structure and excellent intrinsic properties, which has been used as a catalyst to support and enhance the catalytic activity of semiconductor. Here, the typical synthesis methods of 3D GA were summarized, such as hydrothermal, chemical vapor deposition, and chemical oxidation, etc. Furthermore, the application of 3D GA based photocatalyst in the degradation of organic pollutants is reviewed, especially different 3D GA based composite materials and their degradation ability on organic dyes in wastewater as well as their biohazard in the ecosystems is critically discussed. In addition, we discuss the challenges for large scale preparations of 3D GA and further improvement for the degradation efficiency. It is expected that this review would be helpful for designing of highly efficient 3D GA based photocatalyst composites.

## 1. Introduction

Water pollution has become a serious problem in this century

mainly due to the massive and uncontrolled discharge of organic compounds, which lead to the deterioration of clean water and exacerbate the water shortage [1–9]. A variety of organic pollutants, such

\* Corresponding authors at: College of Environmental Science and Engineering, Hunan University, Changsha, 410082, China.

E-mail addresses: [zgming@hnu.edu.cn](mailto:zgming@hnu.edu.cn) (G. Zeng), [yuelu@hnu.edu.cn](mailto:yuelu@hnu.edu.cn) (Y. Lu).

<sup>1</sup> These authors contributed equally to this work.

as rhodamine B (RhB), methylene blue (MB) and phenolic compounds have been widely used in textile, leather and other industrial manufacture [10]. Over the past few years, more than 100,000 different kinds of organic dyes have been found, and their annual consumption is about 36,000 tons [11]. Unfortunately, wastewater including organic pollutants is one of the most difficult problems to solve. To date, several methods have been developed including adsorption [12–17], coagulation [18] and photocatalysis [19–21], which have been widely applied in the area of organic dyes in sewage [22]. Among numerous techniques, photocatalysis shows advantages in the following aspects: gentle pH value of solution, mild reaction temperature, and high efficiency [23]. Compared with other carbonaceous materials, the graphene has some unique advantages [24,25]. Hasija et al. summarized noble metal free doped g-C<sub>3</sub>N<sub>4</sub> photocatalysts for water purification with defects such as wide band-gap, small specific surface area, and high electron-hole recombination rate, which leads to lower degradation rate [26]. Sharma et al. raised CQDs as electron mediator to enhance the photocatalytic activity of semiconductor [27]. They also reported PGCN/AgI/ZnO/CQD composite via the hydrothermal method with bamboo leaves [28]. Although remarkable progresses have been made, there are still a number of key pathways that hinder the practical application of photocatalysis in organic pollutant wastewater treatment, especially in the selection of high efficiency photocatalysts. Adsorption capacity of contaminants plays a critical role in photo-degradation process [29]. Graphene has high surface area and displays excellent adsorption capacity and shows potential photocatalytic capacity [30]. Singh et al. summarized graphene-based composite can serve as photocatalysts and disinfectants [31]. Shandilya et al. reported EuVO<sub>4</sub> coupling with F doped graphene sheets presents great degradation property and stability in water purification [32]. S and P co-doped Ag<sub>2</sub>CO<sub>3</sub>/GCN heterojunction photocatalyst was synthesized by Raizada et al. for DNP removal efficiency via accelerated photocatalytic reactions [33].

Recently, three dimensional graphene aerogel materials (3D GA) attracted communities' attention [34] due to its porous structure and excellent intrinsic properties [35]. Furthermore, 3D GA based photocatalysts composite has been recognized as a candidate material to solve these above problems. During the preparation of 3D GA, partially reduced graphene oxide (RGO) was polymerized by van der Waals forces, p-p superposition and a large amount of water hydrogen bonding to form a strongly cross-linked 3D graphene network [36]. The strong crosslinking of 3D GA network may hinder the aggregation of graphene and has abundant mass transfer pores [37]. Therefore, 3D GA can be used as a catalyst support and enhance the practical application potential of graphene in the following aspects: i) it can keep the complete morphology after photocatalytic reaction ; ii) it is easy to operate and separate in practical application; iii) it can prevent the release of graphene nanoparticles and decrease its environmental risk [38,39]. Due to these advantages, compared with graphene nanoparticles, 3D GA has attracted widespread attention with the large increase in 3D GA research articles (Fig. 1).

3D GA has a great potential to deal with the degradation of organic pollutants in wastewater. It should be noted that 3D GA also has a high adsorption capacity for organic pollutants, which will help improve its ability to degrade organic pollutants [40]. Many studies on 3D GA have been published, but a comprehensive review of its application as a low-cost photocatalyst to remove organic dyes in aqueous environments has not been reported [41]. In this paper, the research progress of 3D GA is summarized [42]. Various synthesis methods of 3D GA are briefly introduced. Then, different 3D GA based photocatalysts as catalysts in the environmental remediation are concluded. Environmental impact of 3D GA is discussed. Finally, the challenge and perspectives for future development are discussed. We hope that this paper would be helpful for the designing and fabricating novel 3D GA based photocatalysts with better performances in the near future.

## 2. Synthesis methods of 3D GA

Compared with the strict definition of monolayer graphene, 3D GA mainly contains multilayer carbon atoms. 3D structure makes the progress of its synthesis more difficult. In order to satisfy the requirement of application in organic dyes pollutants removal, it is imperative to develop simple and efficient preparation methods. So far, the general synthetic strategies reported in the literatures can be mainly classified into several categories, including oxidation-reduction approach [43,44], template-directed approach [45], chemical vapor deposition approach [46], electrochemical synthesis approach [47] and other approaches. Oxidation-reduction is the most common method. Firstly, 3D GA can be produced in quantity. Secondly, the reaction conditions are relatively simple [48]. However, the chemical reduction method has the advantages of simple reaction device, mild reaction conditions, and easier to achieve large-scale production. Compared with the oxidation-reduction method [49], chemical vapor deposition [50] and electrochemical reduction assembly has the advantages of fast reaction speed, simple and easy to control [51]. According to different crosslinking methods, it can be divided into physical crosslinking and chemical crosslinking. The method of physical crosslinking can prepare GA under mild conditions, but the physical crosslinking GA have low stability and poor mechanical properties. The hydrothermal reduction method avoids the introduction of non-carbon impurities because it does not use binders and chemical additives. It is easy to operate, but the reaction environment is relatively harsh [52]. In addition, from the economic point of view, the secondary pollution by the redox method needs treated. The freeze-drying involved in the operation is not economical, and the drying at room temperature and pressure is more suitable for industrialization. This section mainly introduces the common methods of synthesizing 3D GA.

### 2.1. Hydrothermal reduction

In the past decade, hydrothermal reduction method has been found to be an effective strategy for synthesized 3D GH [53,54]. 3D GA is obtained by dehydrating of 3D GH (Fig. 2) [55]. Cross-linking agents such as polymer [52,56], metal ions [57,58] were added into the GO dispersions to form 3D GH. 3D GA can be obtained through direct freeze-drying [59], electrochemical deposition [60,61] and centrifugation. Freeze-drying method is the most commonly used method due to its simple operation and easy conditions [62]. Yang et al. prepared 3D GA composite by mixed WO<sub>3</sub> with GO solution with freeze-drying for 48 h. The results indicated that 3D GA can serve as a support, improve light absorption, increase the catalyst surface area (from 46 to 57 m<sup>2</sup> g<sup>-1</sup>), and promote the separation efficiency of charge carriers [63].

Self-assembling based on the traditional hydrothermal reduction method is a new way that caused much concern. Wu et al. [64] proposed a new method to prepare self-assembled graphene hydrogel (GHS) that interconnects three-dimensional networks with Cu nanoparticles. With this method, Cu (I) oxides were deposited on reduced graphene oxide thin films and embedded in GHS (Fig. 3), and then GHS was converted into 3D GA by freeze-drying method. The composition of 3D GA can be conveniently adjusted by changing the initial amount of Cu nanoparticles or the concentration of GO suspensions. This method can be used to promote the conversion of some parts of GO to RGO via the oxidation of metal ions. The results exhibited that the structure stability shows a trend of first high and then low and more particles appear on graphene wafer with the increase of the initial amount of metal nanoparticles (Fig. 4). In addition to copper ion, other oxidized metal ions, e.g. Fe<sub>3</sub>O<sub>4</sub> [65], and Fe<sub>2</sub>O<sub>3</sub> also have the function of forming three-dimensional network structure as crosslinking agents, which proved the validity of using metal ions as a crosslinking agent.

Besides metal ions, there are some other cross-linking agents which can form 3D GA. Hydrothermal reduction method has been proved to

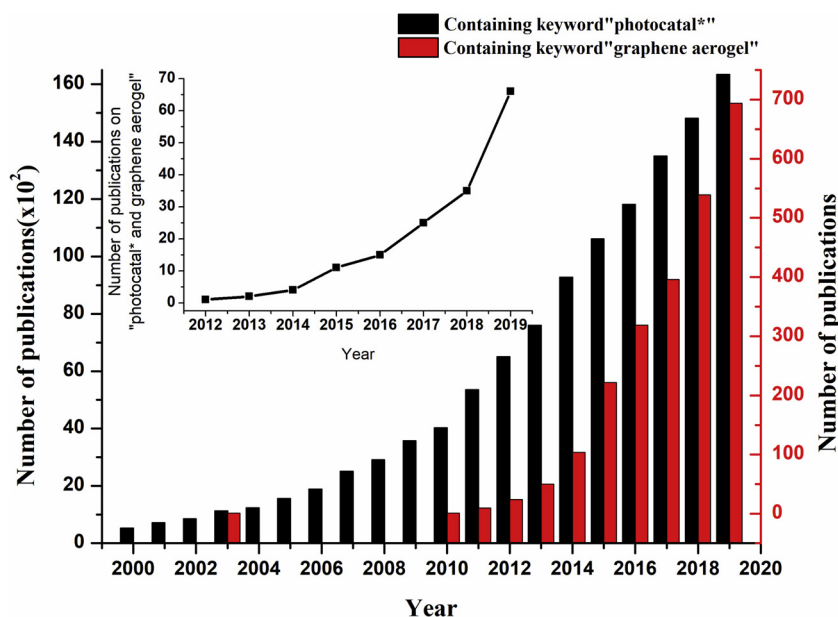


Fig. 1. Numbers of yearly publications about photocatalyst for wastewater since 2000, the inset shows the number of papers published per year on graphene aerogel-based photocatalyst since 2000 from web of science.

be an effective method for the synthesis of 3D GA. This method has its limitations, such as the production of many harmful by-products, acidic waste liquid, etc. In addition, how to choose a cross-linking agent and control the reaction conditions is another problem.

## 2.2. Chemical vapor deposition (CVD) of 3D GA

Template guidance is another effective method to construct 3D graphene structures. Template guidance method can generate a three-dimensional porous graphene network with any specific shape and structure of 3D scaffold or layered membrane [66], which is helpful to improve the fast electron transfer between active material and collector. This method is helpful for the synthesis of graphene with large size, controllable shape [67,68]. The size of 3D GA synthesized in this way depends on the substrate material of template and the control of experimental temperature. In principle, CVD is template guidance. Chen et al. [48] have proved that the template guiding CVD method is an effective method for the synthesis of graphene foam (GFs) with three-dimensional microjunction (Fig. 5).

In this method, highly interconnected nickel from three-dimensional scaffolds is used as a sacrificial template to grow wrinkled graphite films by decomposing methane ( $\text{CH}_4$ ) at 1000 °C on atmospheric

pressure. After etching the bottom nickel with inorganic acid, a continuous, interrelated 3D GF was obtained, which has ultralow density of  $5 \text{ mg cm}^{-3}$  and high specific surface area up to  $850 \text{ m}^2 \text{ g}^{-1}$ . The GF made by this method is a whole 3D network graphene, which is different from the 3D structure formed by the small CMG chip. Its medium charge carriers can pass through the structure of high quality continuous graphene grown by CVD and move rapidly with small resistance. This CVD method showed great versatility in controlling graphene frame structure. For example, the size and pore structure of GFs can be adjusted by using different nickel foams, while the average number of the layers, the specific surface area and the density of GFs can be controlled by changing the concentration of  $\text{CH}_4$ . Besides, cellulose nanofiber (CNF), was used as a raw material dispersant and modified with CVD technique to obtain super-hydrophobic aerogels with low density and high porosity in the other fields [69].

## 2.3. Chemical reduction method of 3D GA

Compared to hydrothermal reduction that need cross-linkings, inert gas at high temperatures or a reducing environment [70], chemical reduction is simpler, which generally use a convenient reductant, such as hydrazine, Vitamin C, sodium ascorbate and other reagents [71–74].

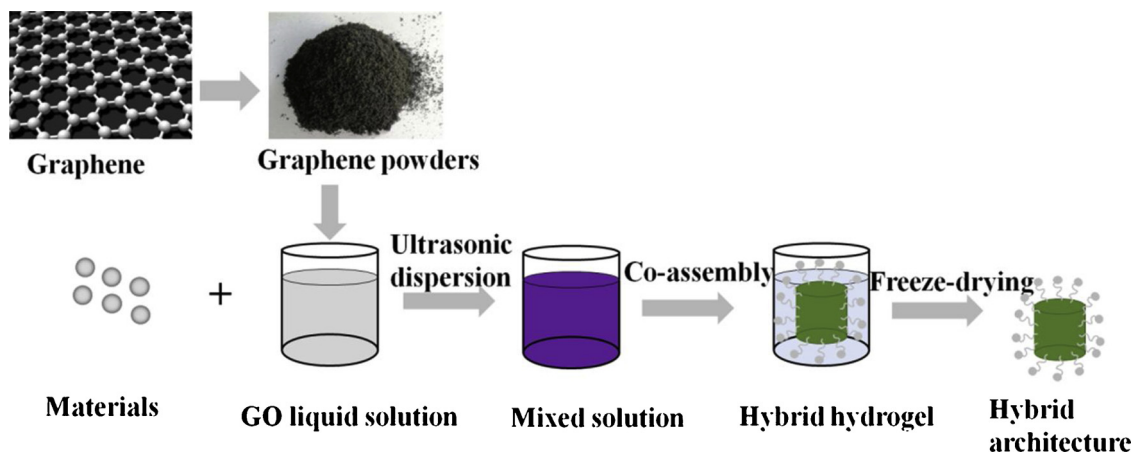
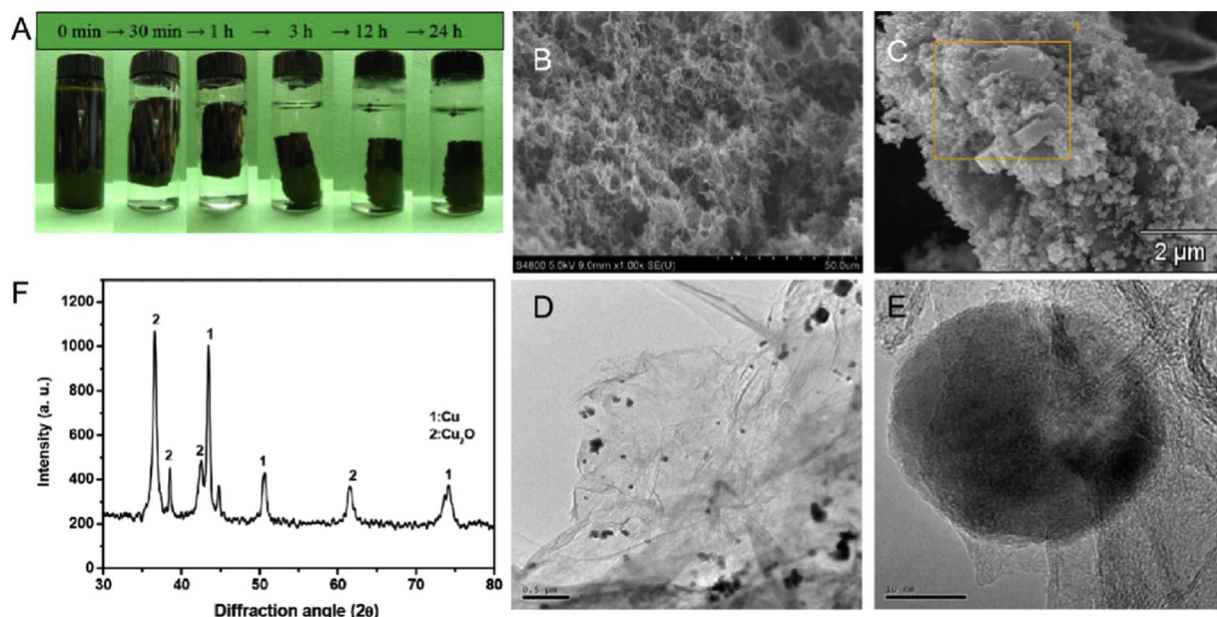


Fig. 2. 3D GA prepared by hydrothermal reduction process.



**Fig. 3.** (A) Photographs of the formation process for the graphene hydrogels with 25 mL of GO suspension (2 mg/mL) in the presence of Cu (0.1 g); (B) Low- and (C) high-magnification SEM images; (D) TEM and (E) high-resolution TEM images of the graphene hydrogel; (F) XRD pattern of the prepared aerogel. Reprinted with permission from Ref. [65]. Published by Journal of Materials Chemistry A.

Besides that, the reductant of the chemical reduction can also be acid or base [75,76].

Chen et al. [77] showed a one-step chemical reduction process that combines GO with hydroiodic acid as the reductant to obtain 3D GA. However, during the reduction process of the graphene-based materials, graphite layers fold due to the  $\pi$ - $\pi$  interactions, leading to a decrease of the specific surface area of the material. Compared with the hydrothermal method, chemical vapor deposition and electrochemical synthesis methods are more environmentally friendly.

### 3. Application of 3D GA based-photocatalysts in the treatment of organic pollutants

In recent years, photocatalysis with inexhaustible solar energy for organic dyes in wastewater has been widely implemented and applied in practical applications. However, in the past years, the traditional photocatalytic powder has defects like low efficiency in the recovery

process. In order to realize the application of photocatalyst in practical application and reduce the overall production cost, fixing the photocatalyst on the suitable support is an important step. Therefore, GA photocatalyst has become a new type of high-efficient recoverable photocatalyst.

The key steps to create the unique macroscopic structure and porous properties of 3D GA in the photoredox catalysis process are absorption, charge separation and transfer, and the role of active material have been proved in the production of 3D GA [78]. The role of 3D GA in photocatalytic oxidation catalysis is diverse (Fig. 6). Firstly, 3D GA has favorable conductivity and multi-dimensional electron transmission path, so it can be used as an ideal optoelectronic medium to promote the separation of photogenerated electron-hole pairs. In addition, the porous structure and abundant surface functional groups make 3D GA as a template to inhibit the aggregation and overgrowth of semi-conductors, thus exposing more active sites for catalytic surface reactions. 3D GA can be directly used as photocatalysts to produce thermal

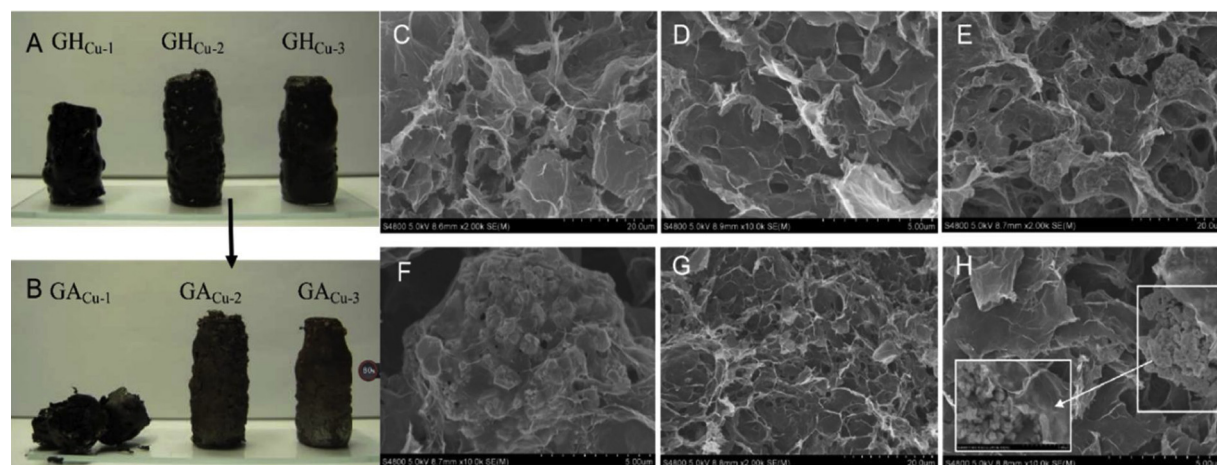


**Fig. 4.** Photographs of (A) GHs and (B) corresponding aerogels dried from the hydrogels prepared using different amounts of Cu nanoparticles. The amount of Cu used for preparation of GHCu-1 -GHCu-3 shown in (A) and (B) was 0.01, 0.05 and 0.1 g. SEM images of the GAs using different amounts of Cu nanoparticles: (C, D) 0.01 g; (E, F) 0.05 g; (G, H) 0.1 g. The inset in F is a high resolution SEM image of Sample GACu-3. (I) the Raman spectra of GAs with 0.01 and 0.1 g. Reprinted with permission from Ref. [65]. Published by Journal of Materials Chemistry A.

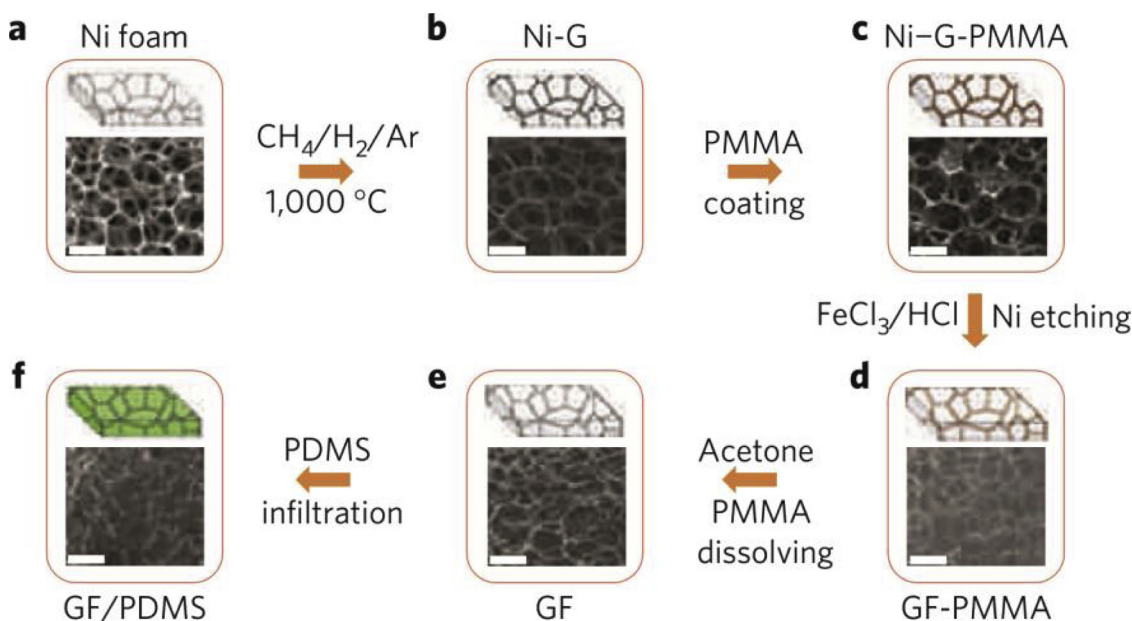


Fig. 5. Flow chart of template directed CVD method. Reprinted with permission from Ref. [48]. Published by Nature materials.

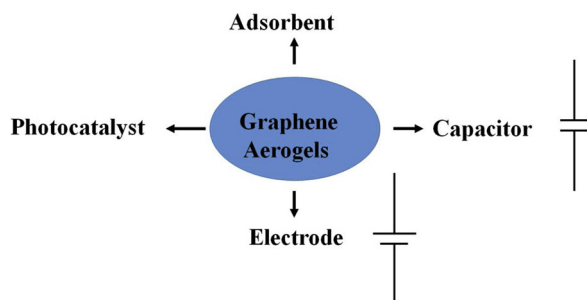


Fig. 6. Four directions in the application of graphene aerogel.

free electrons under light [79].

The excellent adsorption ability and unique monolayer structure of 3D GA can be achieved via constructing composite photocatalyst [80]. As shown in Fig. 7, one strategy is to combine prefabricated 3D GA with photoactive components (e.g. semiconductors), which is the most common method used in the field of organic pollutants degradation. The other strategy is to mix the precursors of GR (e.g. GO) with the soluble precursors of photoactive materials (such as metal salts) and then further process to form 3D GA-based composite photocatalysts.

In this section, we will demonstrate the application of photocatalysts based on 3D GA in eliminating organic matter in water (Fig. 8), including metal semiconductor aerogel photocatalyst, carbon-nitrogen composite photocatalyst and other composite photocatalyst.

### 3.1. 3D GA/metal oxide photocatalysts composite

In this process, GA accelerates the separation of photoelectrons from vacancies, promotes the electron transfer, thus improving the degradation efficiency. In recent years, semiconductor heterojunction photocatalyst (SHPS) has achieved many important research results [81]. Similar with nano CuO/carbon nanotube composites, a C@TiO<sub>2</sub> catalyst was also developed [82–85].

#### 3.1.1. Fundamental principles of 3D GA/metal oxide heterojunction photocatalysts

Due to the development of photocatalytic condition and enhancement of semiconductor heterojunction structure, photocatalysis is more favorable when combined with graphene and 3D GA [85]. From a

photochemical point of view, semiconductor photocatalysts initiate oxidation and reduction reactions under light radiation (Fig. 9). Better crystalline and fewer defects can usually minimize the trapping state and recombination sites, thus improving the efficiency of photo-generated charge carriers for the required light reactions. In the following section, the preparation and applications of 3D GA semiconductor in the removal of organic dyes in wastewater will be described and critically discussed.

#### 3.1.2. 3D GA/metal oxide photocatalysts for organic pollutants degradation

Recently, 3D GA and other semiconductor materials have been applied in surface modification [86–88]. Typically, 3D GA-based semiconductor systems showed higher pollutants adsorption ability, wider light absorption range, quicker charge separation and mass transfer, and thus they favor in improving the degradation efficiency of photocatalyst [89,90]. The comparison of different typical 3D GA-based semiconductor composites for pollutants degradation was listed in Tables 1 and 2.

Zhang et al. [91] prepared 3D GA/TiO<sub>2</sub> composites via a facile one-pot route. The result shows that optimized sample exhibits the best performance of RhB removal and the final degradation rate is as high as 98.7%. After five successive cycles, the degradation rate is still in 70.0%. The results imply that the TiO<sub>2</sub>-GA composites are efficient in the removal of organic pollutants.

Yu et al. fabricated 3D GA/BiOBr using a two-step hydrothermal method [92]. The 3D GA/BiOBr exhibited a much higher reaction rate constant than pure BiOBr [93,94]. Among them, 3D GA/BiOBr with RGO weight ratios of 10 wt% sample showed the highest photocatalytic activity, which was 3.5 times that of pure BiOBr [95].

After that, Liu et al. also proposed a brief one-step solvothermal method to obtain 3D GA/Bi<sub>2</sub>MoO<sub>6</sub>, which made Bi<sub>2</sub>MoO<sub>6</sub> (BMO), an efficient photocatalysts with a controllable size, uniformly distributed in the 3D porous structure [96]. The photocatalytic rate of 3D GA/Bi<sub>2</sub>MoO<sub>6</sub> for MB removal was about 2.1 times higher than BMO, which reached up 98.3% in 100 min. Zhang et al. [97] synthesized Fe<sub>2</sub>O<sub>3</sub>-TiO<sub>2</sub>-GA magnetic photocatalyst by one-step hydrothermal method and freeze-drying method, which prevented the agglomeration of other nanoparticles in the recovery process to some extent. And the metal-metal heterojunction structure of Fe<sub>2</sub>O<sub>3</sub>-GA was formed with TiO<sub>2</sub>. The experimental results show that the adsorption and degradation efficiency of RhB dye by 25 wt% Fe<sub>2</sub>O<sub>3</sub>-GA is the highest (97.7%). After 4

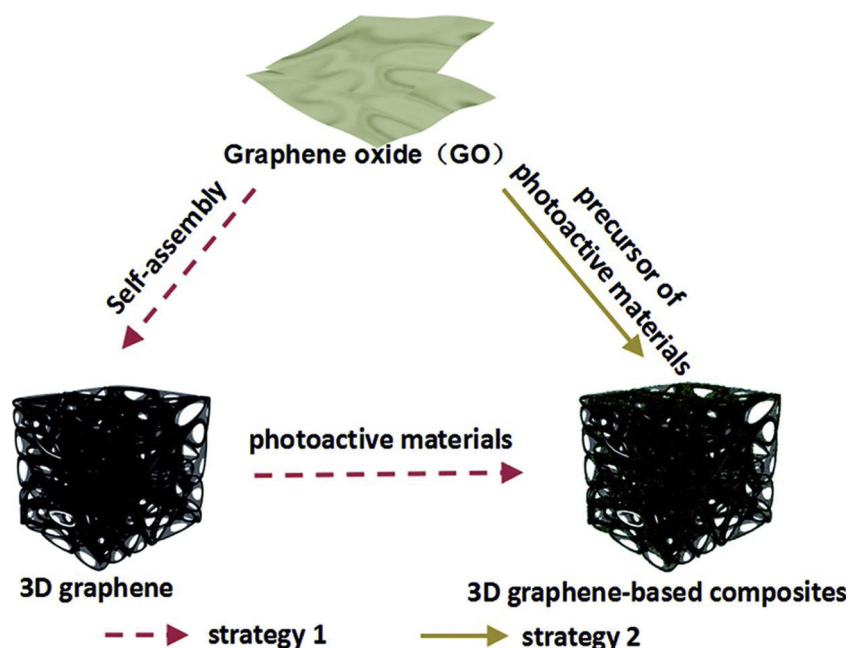


Fig. 7. Schematic illustration of the fabrication strategies of 3D GA-based photocatalysts. Reprinted with permission from Ref. [34]. Published by Journal of Materials Chemistry A.

cycles, the removal rate remained above 81.8 %. This showed that the 3D GA semiconductor composite had positive visible light-driven photocatalytic activity for the removal of organic pollutants.

### 3.2. 3D GA/ $g\text{-C}_3\text{N}_4$ photocatalysts

Recently,  $g\text{-C}_3\text{N}_4$  is a very attractive photocatalyst for organic pollutants degradation since it absorbs visible light [98]. In particular,  $g\text{-C}_3\text{N}_4$  has excellent chemical stability and a promising application prospect in the field of photocatalysis. However, high electron hole recombination, low specific surface area and low photo absorption efficiency largely limit its catalytic performance. To overcome these shortcomings,  $g\text{-C}_3\text{N}_4/\text{GA}$  with the synergistic effect of  $g\text{-C}_3\text{N}_4$  and GA provided a new feasible solution for visible light catalyst with high performance. In particular, the good conductivity of GA inhibited the electron-hole recombination of  $g\text{-C}_3\text{N}_4$  and improved the utilization rate of visible light by multiple light reflections on the connected open skeleton [99].

3D GA/ $g\text{-C}_3\text{N}_4$  (CNGA) was prepared via simple hydrothermal

method as reported by Tong et al. [100]. The morphology, structure and properties of 3D GA,  $g\text{-C}_3\text{N}_4$  nanoparticles and CNGA were characterized in details. 3D GA/ $g\text{-C}_3\text{N}_4$  composite has strong mechanical resilience under complex hydrological conditions and is suitable for photocatalyst restoration. The composite has a connected, porous 3D GO structure and crystalline CN exists in it (Fig. 10). Crystalline CN has graphitization construction, high thermal and chemical stability, and semiconductor electronic structure [101], which can promote the treatment of catalytic reaction.

Wan et al. conveniently prepared  $\text{C}_3\text{N}_4/\text{GOA}$  by freezing casting  $\text{C}_3\text{N}_4$  and GO together and researched their performance as microscopical photocatalysts with different shapes and sizes [103]. They found that  $\text{C}_3\text{N}_4/\text{GA}$  with extra optical density ( $3\sim 5\text{ mg cm}^{-3}$ ), photochemical properties and high adsorption capacity. Besides, this method can be used in the preparation of other two-dimensional materials (e.g.  $\text{MoS}_2$ , BN)/GA catalysts, which can lay a foundation for the future application of industrial photocatalysis. He et al. also fabricated a ternary 3D aerogel by a two-step facile hydrothermal method. Herein, RGO is regarded as the framework, modified with carbon quantum dots

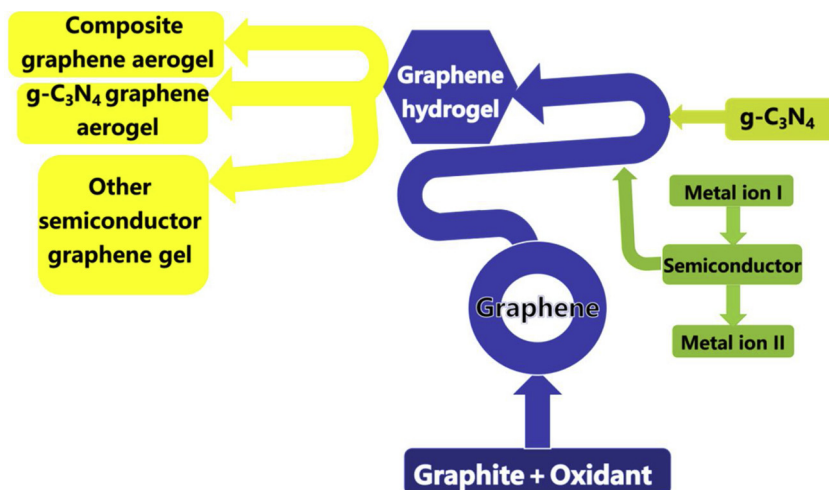
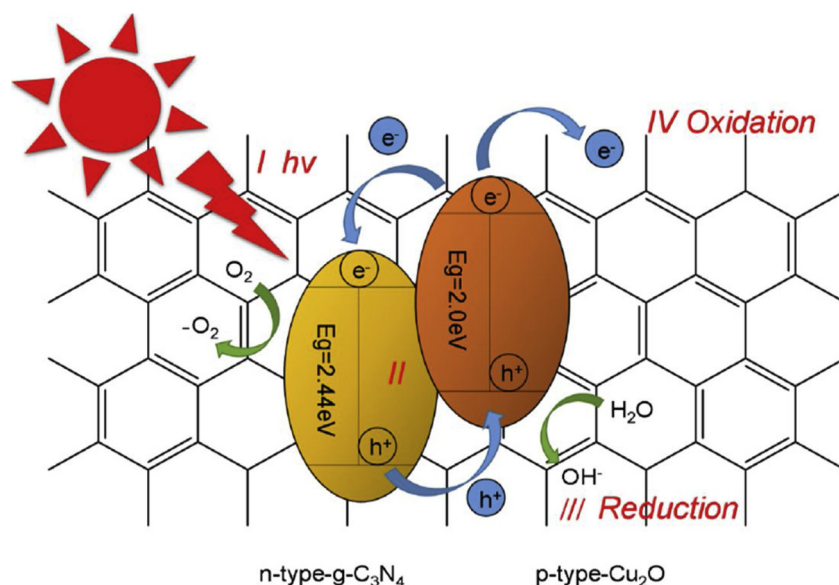


Fig. 8. Study on 3D GA-based photocatalyst.



**Fig. 9.** Schematic diagram of semiconductor photocatalysis principle: (I) the formation of charge carriers by a photon; (II) carriers' recombination to release heat energy; (III) reduction pathway; (IV) oxidation pathway.

and g-C<sub>3</sub>N<sub>4</sub> nanosheet. The degradation removal ratio of MO for this ternary composite was 91.1 % within 4 h, which is 7.6 times than g-C<sub>3</sub>N<sub>4</sub> [104].

Pure graphene is not a photocatalyst actually [105]. However, the N-doping of graphene showed light absorption [106]. The formation of N-Ti-O bonds was similar to the reduced GO, which may lead to the formation of localized states in the band gap of TiO<sub>2</sub> and narrow the band gap [107]. The presence of carbon in graphene derivatives reduced the reflection of light and enhanced the absorption of visible light. The catalytic performance of the coupling of 3D GA with g-C<sub>3</sub>N<sub>4</sub> can be significantly increased by controlling the synergies [108]. Inspired by these works, the multifunctional aerogels with high visible photocatalytic activity and petroleum adsorption ability was obtained by converting C<sub>3</sub>N<sub>4</sub> powder into macro aerogels. This experiment demonstrated that pure nitrogen doping of GA photocatalysts was feasible. Tong et al. evaluated that photocatalytic activity of CNGA samples under visible light irradiation by the degradation of MO (Fig. 11a). The degradation rate of CNGA<sub>2</sub> was the highest, which was about 6.0 times of that of g-C<sub>3</sub>N<sub>4</sub>. At the same time, the loss of photocatalytic activity of CNGA in the four-cycle decomposition process is not obvious (Fig. 11c), which indicates that the metal-free photocatalyst has good stability. Compared with pure g-C<sub>3</sub>N<sub>4</sub>, the degradation efficiency of MO was much higher in all CNGA samples under the same conditions, indicating that there was a synergistic effect between g-C<sub>3</sub>N<sub>4</sub> and GA. Besides, g-C<sub>3</sub>N<sub>4</sub> acted as a photocatalyst in CNGA samples to generate electron-hole pairs under visible light, while GO not only formed a 3D

porous aerogel skeleton, but also facilitated photoelectron transfer. Compared with the composite doped by nitrogen and semiconductor, pure nitrogen modified GA still has a gap in catalytic oxidation.

### 3.3. GA modified by other complex materials

#### 3.3.1. Ternary semiconductors heterojunction

Metal oxide semiconductors (MOS) have advantages of high oxidation ability, low toxicity and positive chemical stability, and they have become ideal materials for the degradation of organic pollutants. However, due to the fast recombination of photo-generated charge carriers, the photocatalytic efficiency remains to be further improved. g-C<sub>3</sub>N<sub>4</sub> with N-bridged triazine repeat units is a kind of metal-free photocatalyst with excellent thermochemical stability, electronic and optical structure [110,111]. Various strategies have been studied, including combination with other semiconductor or carbon materials, doping of metal and/or nonmetallic ions, formation of heterojunction etc [112–115]. Therefore, hybridizing with a suitable support may solve this problem.

For example, Table 1 shows GA-based catalysts, the catalytic rate of g-C<sub>3</sub>N<sub>4</sub>/BiOBr/RGO [116] and g-C<sub>3</sub>N<sub>4</sub>-TiO<sub>2</sub>-GA [117] was 66 % and 98 % in 60 min, respectively, which was much higher than the pure nitrogen doping catalyst because of the stereoscopic layered porous structure and synergism in the ternary system. Similarly, a Cu<sub>2</sub>O/g-C<sub>3</sub>N<sub>4</sub>/GA was prepared by Yang et al. Cu<sub>2</sub>O/g-C<sub>3</sub>N<sub>4</sub>/GA obtained 96 % of MB and 83 % of MO removal efficiency in 80 min, which indicated

**Table 1**

Photocatalytic degradation of RhB Organic Dyes in Water with several graphene aerogel based photocatalysts.

Photocatalyst (mg)	Pollutant (mg/L)	Light source(W)	Degradation	Time (min)	cycle	Cyclic effect	Ref
Ag <sub>2</sub> O/ALG-rGO(30)	RhB(5)	500 W Xe lamp	96 %	150	5	89%	[119]
Bi <sub>2</sub> WO <sub>6</sub> /GA(20)	RhB(10)	300 W Xe lamp	99.6 %	45	ND	ND	[120]
BiOBr/RGO aerogel	RhB	300 W Xe lamp	over 68 %	ND	5	68 %	[121]
CeO <sub>2</sub> /RGA	RhB	150 W Xe lamp	85 %	120	3	No significant changes	[122]
BiOBr/RGO	RhB	300 W Xe lamp	50 %	60	ND	ND	[92]
g-C <sub>3</sub> N <sub>4</sub> -TiO <sub>2</sub> -GA(5)	RhB(20)	500 W Xe lamp	98.40 %	60	4	75.60%	[117]
Fe <sub>2</sub> O <sub>3</sub> -TiO <sub>2</sub> -GA(5)	RhB(20)	500 W Xe lamp	97.70 %	60	4	81.80 %	[97]
W <sub>18</sub> O <sub>49</sub> -RGO	RhB	500 W Xe lamp	100 %	25	30	No significant changes	[123]
TiO <sub>2</sub> -GA(5)	RhB(20)	300 W Xe lamp	98.7 %	180	5	70%	[91]
3D Ag/Ag@Ag <sub>3</sub> PO <sub>4</sub> /GA (7.5)	RhB(15)	400 W Xe lamp	100.0 %	15	6	No significant changes	[124]
3D g-C <sub>3</sub> N <sub>4</sub> /BiOBr/RGO	RhB	300 W Xe lamp	66 %	60	3	No significant changes	[116]

**Table 2**  
Photocatalytic degradation of other organic dyes in Water with several graphene aerogel based photocatalysts.

Photocatalyst(mg)	Pollutant (mg/L)	Light source	Degradation	Time (min)	Ref
Ag <sub>2</sub> O/ALG-rGO(30)	OII (10)	500 W Xe lamp	93 %	60	[119]
CeVO <sub>4</sub> /GA	MB	500 W Xe lamp	98.00 %	18	[129]
TiO <sub>2</sub> /GA	MB	500 W Xe lamp	90 %	30	[130]
TiO <sub>2</sub> /rGO-GA	MO	U-visible light	98 %	240	[131]
BiOBr/RGO	MO	U-visible light	80 %	60	[92]
TiO <sub>2</sub> Nanocrystals/GA	MO	U-visible light	90 %	180	[132]
S-TiO <sub>2</sub> -3DGA(5)	MO(6)	Ultraviolet light	83.9 %	90	[133]
W <sub>18</sub> O <sub>49</sub> -RGO	MO	U-visible light	100.00 %	25	[123]

that the Cu<sub>2</sub>O/g-C<sub>3</sub>N<sub>4</sub> heterojunction based on RGO can enhance visible light absorption [118].

In the description of the relevant literature, as proved by other studies, semiconductor structure had a higher electron transport rate and more reaction sites were exposed in a 3D network with a mesh-like structure, in which nitrogen ions were interdigitated with each other.

### 3.3.2. MOF modified GA

Metal-organic framework (MOF) is a porous crystal material with large specific surface area, ordered arrangement and controllable pore size, which is used for gas storage and water purification, and has a

broad application prospect in catalyst and drug carrier [125]. Roeyffers et al. reported the photocatalytic activity of Fe (III) based MOFs such as MIL-101 (Fe), MIL-100 (Fe) and MIL-88B (Fe) in the decolorization of RhB [126].

However, when MOF is used in separation, absorption and catalytic applications, the stability and reuse of MOF is a major challenge [127]. To solve that, 3D GA provides an ideal mechanical support material. Mao et al. reported a new method about self-assembly of MOFs [128]. Compared with single 3D GA aerogels, ZIF-8/3D GA showed good oil absorption and photocatalytic degradation ability. When ZIF-8/RGA catalyst was added, the concentration of MB decreased rapidly to 51.8

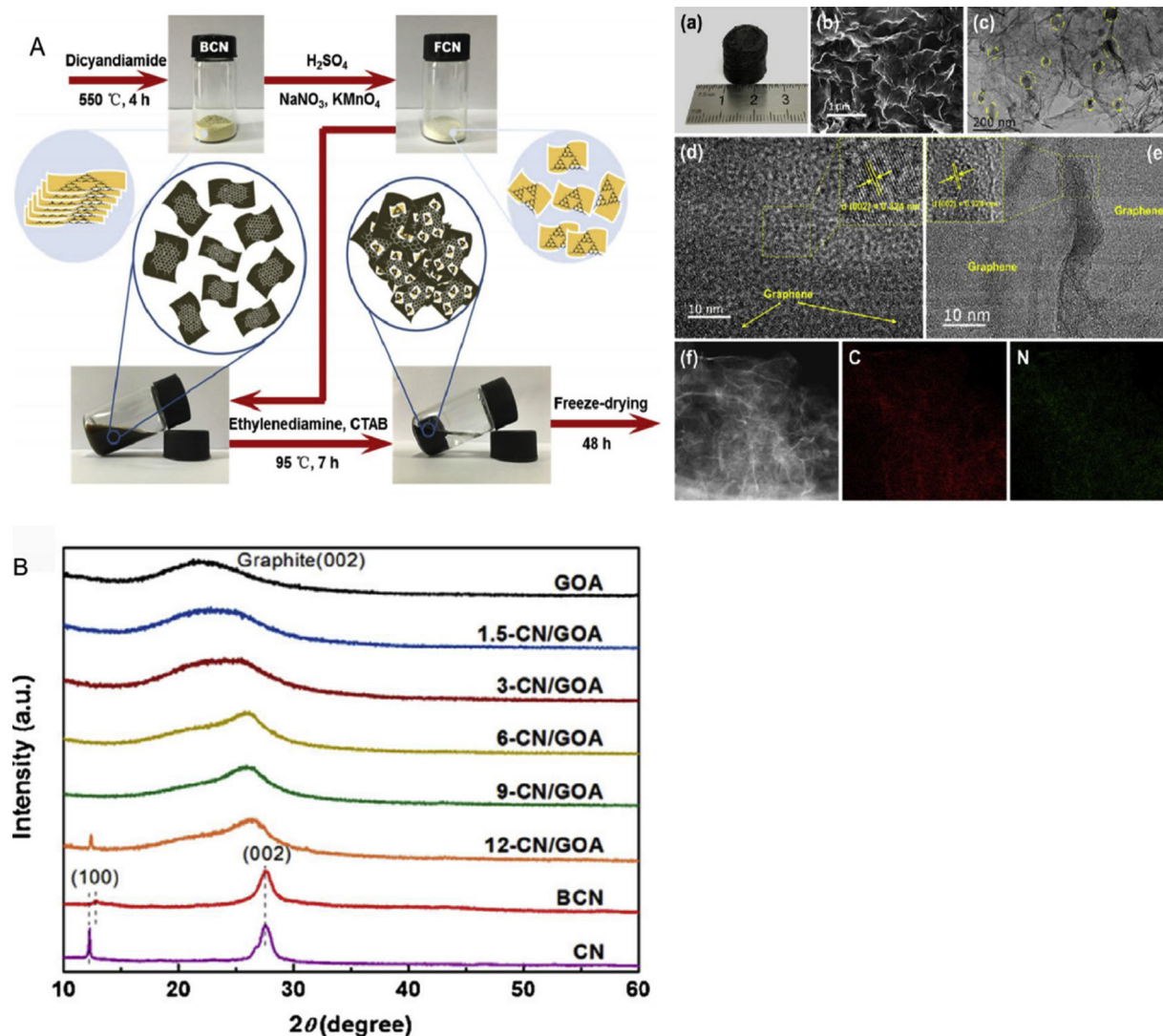


**Fig. 10.** (A) Mechanism of the CN/GOA hybrid synthesis, (a-e) Digital image, SEM image, TEM images and HRTEM images; (f) HAADF image and C and N elemental mapping; (B) XRD patterns of samples. Reprinted with permission from Ref. [102].



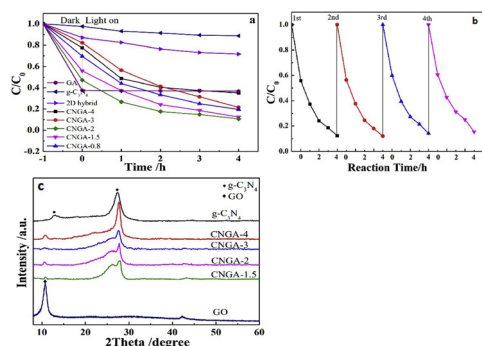


**Fig. 11.** (a) Photocatalytic degradation of MO ( $C_0 = 20 \text{ mg L}^{-1}$ ) under visible light irradiation; (b) Cycle runs of CNGA-2 for MO degradation; (c) XRD patterns of pure g-C<sub>3</sub>N<sub>4</sub>, GO and as-prepared CNGA samples. Reprinted with permission from Ref. [109]. Published by ACS.

%, which indicated that the catalyst had higher degradation efficiency compared to pure 3D GA.

### 3.3.3. Other metal oxide modified GA

Nanowires emerged as a unique composite material. Li et al. prepared a tungsten oxide reduced graphene aerogel ( $W_{18}O_{49}$ -rGA) by a simple hydrothermal method [123]. Compared with pure  $W_{18}O_{49}$  nanowires, the photocatalytic efficiency of the  $W_{18}O_{49}$ -rGA was significantly improved for the degradation of RhB and other five different organic dyes (i.e. reactive black 39, reactive yellow 145, weak acid black BR, methyl orange, and weak acid yellow G.). The results showed that the degradation activity of RhB was 98 % in 15 min. And the photocatalytic efficiency of  $W_{18}O_{49}$ -rGA on six dyes remained above 90 % after 30 cycles.

Nanosheets have been described as another unique composite material. Xu et al. prepared a 3D GA/ $Bi_2WO_6$  by using  $Bi_2WO_6$  nanosheets and RGO as building materials, and the catalytic activity is studied by the degradation of RhB [120]. In the experiments, a series of  $Bi_2WO_6$ /GA(BWGA) composites were prepared by changing the mass fraction of GO in the composites. BWGA-0.03 could completely degrade RhB within 45 min (99.6 % degradation), whereas the  $Bi_2WO_6$  nanosheets degrades 80 % of RhB. In general, nanowires are more efficient than MOFs in the catalytic decomposition of organic dyes in aquatic solution. The main reason is that MOFs material itself has some limitations in the field of catalysis.

## 4. Environmental impact of 3D GA

Graphene is an important raw material for the synthesis of GA. With its growing widespread application in many industries, we cannot ignore its hazards. If graphene nanoparticles enter surface or subsurface water, they have a negative environmental impact due to sharp edges which can hurt cells. Graphene nanoparticles form unstable precipitates in the aquatic environments and therefore are harmful to living microorganisms, plants, animals and humans. A research team from Brown University examined the potential toxicity of graphene material to human cells and jagged edges of graphene nanoparticles were found very sharp and strong, which easily penetrated into human skin as well as the cell membrane of immune cells [134]. Besides, if graphene sheet up to 10 microns, it can be completely absorbed by cells as shown in Fig. 12.

Many studies on the potential toxicity of graphene have been reported. [135]. The toxicity of 3D GA particles *in vivo* mainly depends on their dose and size. Biocompatibility studies using mice showed that intravenous injection of low-dose graphene oxide (0.1 mg) and medium-dose graphene oxide (0.25 mg) did not cause detect toxicity, while high-dose graphene oxide (0.4 mg) resulted in chronic toxicity on mice [136]. In another study, different forms of graphene, such as

polymeric graphene solution, polydisperse graphene solution and graphene oxide solution, were injected directly into the lungs of mice. 3D GA induced mitochondria to produce reactive oxygen species, activated inflammatory and apoptotic pathways, and led to severe and persistent lung injury, while the lung injury of mice treated with graphene aggregation and dispersion was not obvious [137]. Besides, Hui et al. reported that the effects of GA on the body vary with size. Large particles ranging from 1 to 5 microns to 110–500 nm accumulated in the lungs, while smaller particles got trapped in the liver of mice [138]. Furthermore, graphene nanosheets can induce pulmonary inflammation, thromboembolism, and immune responses in mice after being injected into a vein [139]. The over-production of hydroxyl radicals and the formation of oxidizing cytochrome c intermediates is responsible for the toxicity properties.

Even though our knowledge of the toxicology of graphene nanoparticles like GA is still limited. To reduce their environmental risk, one of the feasible solution is the recycle of graphene nanoparticles. It is worth noting that the GA discussed in this review has a reduced environmental hazard due to its good recovery and high elasticity, higher recoverability and recyclability comparing to pure graphene or other types of graphene nanomaterials. Still, more studies are required to assess the environmental risk of graphene nanoparticles like GA, and to reduce their negative impact on the human body and the aquatic ecosystems.

## 5. Summary and outlook

In conclusion, this work summarized recent progress on the synthesis of 3D GA and 3D GA photocatalyst composites. Many methods including hydrothermal, CVD, and chemical oxidation have been explored for their syntheses. GA is a valuable material known for its typical 3D porous skeleton, large specific surface area and high adsorption capacity. With  $\pi$ - $\pi$  interlaminar stacking and hydrogen bonding, GA has high interconnection, good conductivity and other valuable characteristics. 3D GA photocatalyst has been applied in photocatalytic degradation of organic pollutants. Coupling 3D GA with semiconductors can dramatically improve the photocatalytic activity.

Despite the bright future of 3D GA-based materials, there are some issues should be taken into consideration:

- (1) Compared with traditional GA modification methods, composite modified GA based photocatalyst has a great advantage in the wastewater treatment, but the corresponding cost is also higher. The next step is to improve the experimental process of GA based photocatalyst via proper modification methods like nanowire porous nanoplate. And the cost can be reduced via recycling materials and improving test methods.
- (2) For commercial applications, 3D GA has good recyclability, however, the cost of the instrument in the operation steps and potential secondary pollution still need to concern. In the synthesis process, the energy consumption for making graphene aerogels should be reduced. For example, freeze-drying is not economical, while drying at normal temperature and pressure is more suitable for industrialization.
- (3) Additionally, the threat to local ecosystems caused by GA based photocatalyst needs further attention. Graphene molecules can damage the cell tissues of plants and animals, and precipitate with heavy metals. Therefore, trace, estimate and control of the 3D GA-based photocatalysts in the ecosystem and environments are required.

### Declaration of Competing Interest

The authors declare that they have no known competing financial interests or personal relationships that could have appeared to influence the work reported in this paper.

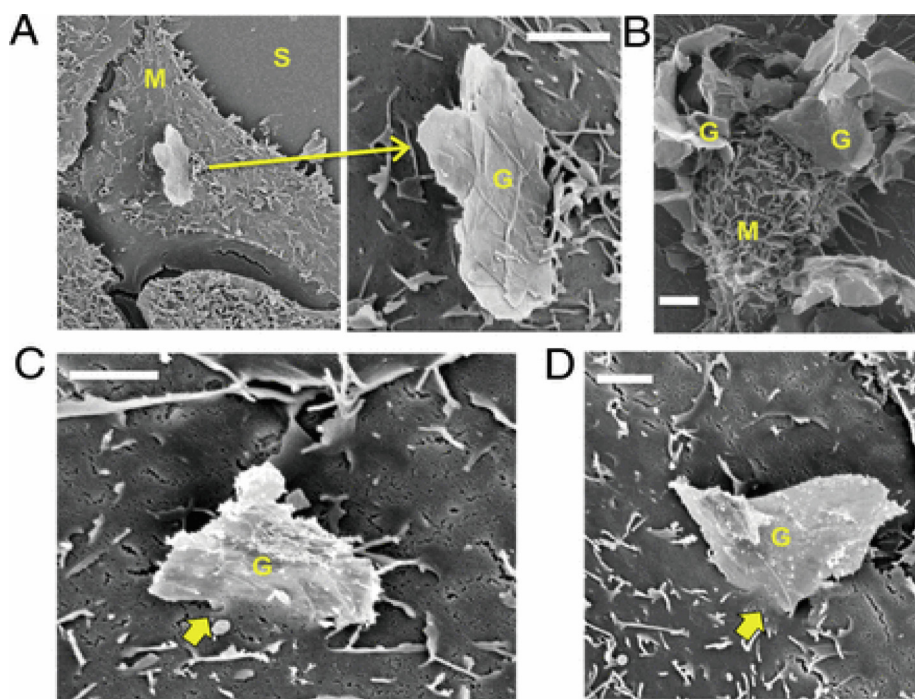


**Fig. 12.** Effects of graphene particles on biological cell membrane: a case study of three cell types (A) The surface of human lung epithelial cells was penetrated by graphene microfragments. (B) Graphene microchip (G) penetrated into the edge of macrophage (M). (C) Interaction between G and primary human keratinocytes, the edges of G appear to have entered the nucleus at rough or prominent locations. Reprinted with permission from Ref. [134]. Published by the National Academy of Sciences.

## Acknowledgements

The study was financially supported by Projects 51709100f National Natural Science Foundation of China, Shanghai Tongji Gao Tingyao Environmental Science and Technology Development Foundation, and the Program for Changjiang Scholars and Innovative Research Team in University (IRT-13R17).

## References

- [1] L. Zhang, J. Zhang, G. Zeng, H. Dong, Y. Chen, C. Huang, Y. Zhu, R. Xu, Y. Cheng, K. Hou, Multivariate relationships between microbial communities and environmental variables during co-composting of sewage sludge and agricultural waste in the presence of PVP-AgNPs, *Bioresour. Technol.* 261 (2018) 10–18.
- [2] Y. Wang, Y. Zhu, Y. Hu, G. Zeng, Y. Zhang, C. Zhang, C. Feng, How to construct DNA hydrogels for environmental applications: advanced water treatment and environmental analysis, *Small* 14 (2018) 1703305.
- [3] X. Tang, G. Zeng, C. Fan, M. Zhou, L. Tang, J. Zhu, J. Wan, D. Huang, M. Chen, P. Xu, Chromosomal expression of CadR on *Pseudomonas aeruginosa* for the removal of Cd (II) from aqueous solutions, *Sci. Total Environ.* 636 (2018) 1355–1361.
- [4] B. Song, P. Xu, G. Zeng, J. Gong, X. Wang, J. Yan, S. Wang, P. Zhang, W. Cao, S. Ye, Modeling the transport of sodium dodecyl benzene sulfonate in riverine sediment in the presence of multi-walled carbon nanotubes, *Water Res.* 129 (2018) 20–28.
- [5] Z. Huang, K. He, Z. Song, G. Zeng, A. Chen, L. Yuan, H. Li, L. Hu, Z. Guo, G. Chen, Antioxidative response of *Phanerochaete chrysosporium* against silver nanoparticle-induced toxicity and its potential mechanism, *Chemosphere* 211 (2018) 573–583.
- [6] L. Qin, G. Zeng, C. Lai, D. Huang, P. Xu, C. Zhang, M. Cheng, X. Liu, S. Liu, B. Li, “Gold rush” in modern science: fabrication strategies and typical advanced applications of gold nanoparticles in sensing, *Coordination Chem. Rev.* 359 (2018) 1–31.
- [7] S. Ye, G. Zeng, H. Wu, C. Zhang, J. Liang, J. Dai, Z. Liu, W. Xiong, J. Wan, P. Xu, Co-occurrence and interactions of pollutants, and their impacts on soil remediation—a review, *Crit. Rev. Environ. Sci. Technol.* 47 (2017) 1528–1553.
- [8] G. Xie, K. Zhang, B. Guo, Q. Liu, L. Fang, J.R. Gong, Graphene-based materials for hydrogen generation from light-driven water splitting, *Adv. Mater.* 25 (2013) 3820–3839.
- [9] P.A.K. Reddy, P.V.L. Reddy, E. Kwon, K.-H. Kim, T. Akter, S. Kalagara, Recent advances in photocatalytic treatment of pollutants in aqueous media, *Environ. Inter.* 91 (2016) 94–103.
- [10] M. Cheng, G. Zeng, D. Huang, C. Lai, Y. Liu, C. Zhang, R. Wang, L. Qin, W. Xue, B. Song, High adsorption of methylene blue by salicylic acid-methanol modified steel converter slag and evaluation of its mechanism, *J. Colloid Interface Sci.* 515 (2018) 232–239.
- [11] K.M. Reza, A. Kurny, F. Gulshan, Parameters affecting the photocatalytic degradation of dyes using TiO<sub>2</sub>: a review, *Appl. Water Sci.* 7 (2017) 1569–1578.
- [12] Y. Liu, M. Cheng, Z. Liu, G. Zeng, H. Zhong, M. Chen, C. Zhou, W. Xiong, B. Shao, B. Song, Heterogeneous Fenton-like catalyst for treatment of rhamnolipid-solubilized hexadecane wastewater, *Chemosphere* 236 (2019) 124387.
- [13] J.-H. Deng, X.-R. Zhang, G.-M. Zeng, J.-L. Gong, Q.-Y. Niu, J. Liang, Simultaneous removal of Cd (II) and ionic dyes from aqueous solution using magnetic graphene oxide nanocomposite as an adsorbent, *Chem. Eng. J.* 226 (2013) 189–200.
- [14] P. Xu, G.M. Zeng, D.L. Huang, C.L. Feng, S. Hu, M.H. Zhao, C. Lai, Z. Wei, C. Huang, G.X. Xie, Use of iron oxide nanomaterials in wastewater treatment: a review, *Sci. Total Environ.* 424 (2012) 1–10.
- [15] X. Tan, Y. Liu, G. Zeng, X. Wang, X. Hu, Y. Gu, Z. Yang, Application of biochar for the removal of pollutants from aqueous solutions, *Chemosphere* 125 (2015) 70–85.
- [16] J.-L. Gong, B. Wang, G.-M. Zeng, C.-P. Yang, C.-G. Niu, Q.-Y. Niu, W.-J. Zhou, Y. Liang, Removal of cationic dyes from aqueous solution using magnetic multi-wall carbon nanotube nanocomposite as adsorbent, *J. Hazard. Mater.* 164 (2009) 1517–1522.
- [17] W. Xiong, Z. Zeng, X. Li, G. Zeng, R. Xiao, Z. Yang, Y. Zhou, C. Zhang, M. Cheng, L. Hu, Multi-walled carbon nanotube/amino-functionalized MIL-53 (Fe) composites: remarkable adsorptive removal of antibiotics from aqueous solutions, *Chemosphere* 210 (2018) 1061–1069.
- [18] B. Shi, G. Li, D. Wang, C. Feng, H. Tang, Removal of direct dyes by coagulation: the performance of preformed polymeric aluminum species, *J. Hazard. Mater.* 143 (2007) 567–574.
- [19] R. Khan, P. Bhawana, M. Fulekar, Microbial decolorization and degradation of synthetic dyes: a review, *Rev. Environ. Sci. Biotechnol.* 12 (2013) 75–97.
- [20] X. Ren, G. Zeng, L. Tang, J. Wang, J. Wan, Y. Liu, J. Yu, H. Yi, S. Ye, R. Deng, Sorption, transport and biodegradation—an insight into bioavailability of persistent organic pollutants in soil, *Sci. Total Environ.* 610 (2018) 1154–1163.
- [21] S. Ye, G. Zeng, H. Wu, C. Zhang, J. Dai, J. Liang, J. Yu, X. Ren, H. Yi, M. Cheng, Biological technologies for the remediation of co-contaminated soil, *Crit. Rev. Biotechnol.* 37 (2017) 1062–1076.
- [22] K. He, G. Chen, G. Zeng, A. Chen, Z. Huang, J. Shi, T. Huang, M. Peng, L. Hu, Three-dimensional graphene supported catalysts for organic dyes degradation, *Appl. Catal. B: Environ.* 228 (2018) 19–28.
- [23] A. Khataee, M.B. Kasiri, Photocatalytic degradation of organic dyes in the presence of nanostructured titanium dioxide: influence of the chemical structure of dyes, *J. Mol. Catal. A Chem.* 328 (2010) 8–26.
- [24] P. Raizada, A. Sudhaik, P. Singh, P. Shandilya, A.K. Saini, V.K. Gupta, J.-H. Lim, H. Jung, A. Hosseini-Bandegharai, Fabrication of Ag<sub>3</sub>VO<sub>4</sub> decorated phosphorus and sulphur co-doped graphitic carbon nitride as a high-dispersed photocatalyst for phenol mineralization and *E. coli* disinfection, *Sep. Purif. Technol.* 212 (2019) 887–900.
- [25] P. Raizada, A. Sudhaik, P. Singh, A. Hosseini-Bandegharai, P. Thakur, Converting type II AgBr/VO into ternary Z scheme photocatalyst via coupling with phosphorus doped g-C<sub>3</sub>N<sub>4</sub> for enhanced photocatalytic activity, *Sep. Purif. Technol.* 227 (2019) 115692.
- [26] V. Hasija, P. Raizada, A. Sudhaik, K. Sharma, A. Kumar, P. Singh, S.B. Jonnalagadda, V.K. Thakur, Recent advances in noble metal free doped graphitic carbon nitride based nanohybrids for photocatalysis of organic contaminants in water: a review, *Appl. Mater. Today* 15 (2019) 494–524.
- [27] S. Sharma, V. Dutta, P. Singh, P. Raizada, A. Rahmani-Sani, A. Hosseini-Bandegharai, V.K. Thakur, Carbon quantum dot supported semiconductor photocatalysts for efficient degradation of organic pollutants in water: a review, *J. Cleaner Prod.* 228 (2019) 755–769.
- [28] V. Hasija, A. Sudhaik, P. Raizada, A. Hosseini-Bandegharai, P. Singh, Carbon quantum dots supported AgI/ZnO/phosphorus doped graphitic carbon nitride as

- Z-scheme photocatalyst for efficient photodegradation of 2, 4-dinitrophenol, *J. Environ. Chem. Eng.* 7 (2019) 103272.
- [29] P. Shandilya, D. Mittal, M. Soni, P. Raizada, A. Hosseini-Bandegharai, A.K. Saini, P. Singh, Fabrication of fluorine doped graphene and  $\text{SmVO}_4$  based dispersed and adsorptive photocatalyst for abatement of phenolic compounds from water and bacterial disinfection, *J. Cleaner Prod.* 203 (2018) 386–399.
- [30] P. Shandilya, D. Mittal, A. Sudhaik, M. Soni, P. Raizada, A.K. Saini, P. Singh,  $\text{GdVO}_4$  modified fluorine doped graphene nanosheets as dispersed photocatalyst for mitigation of phenolic compounds in aqueous environment and bacterial disinfection, *Sep. Purif. Technol.* 210 (2019) 804–816.
- [31] P. Singh, P. Shandilya, P. Raizada, A. Sudhaik, A. Rahmani-Sani, A. Hosseini-Bandegharai, Review on various strategies for enhancing photocatalytic activity of graphene based nanocomposites for water purification, *Arabian J. Chem.* 13 (2020) 3498–3520.
- [32] P. Shandilya, D. Mittal, M. Soni, P. Raizada, J.-H. Lim, D.Y. Jeong, R.P. Dewedi, A.K. Saini, P. Singh, Islanding of  $\text{EuVO}_4$  on high-dispersed fluorine doped few layered graphene sheets for efficient photocatalytic mineralization of phenolic compounds and bacterial disinfection, *J. Taiwan Inst. Chem. E* 93 (2018) 528–542.
- [33] P. Raizada, A. Sudhaik, P. Singh, P. Shandilya, P. Thakur, H. Jung, Visible light assisted photodegradation of 2,4-dinitrophenol using  $\text{Ag}_2\text{CO}_3$  loaded phosphorus and sulphur co-doped graphitic carbon nitride nanosheets in simulated wastewater, *Arabian J. Chem.* 13 (2020) 3196–3209.
- [34] K.-Q. Lu, X. Xin, N. Zhang, Z.-R. Tang, Y.-J. Xu, Photoredox catalysis over graphene aerogel-supported composites, *J. Mater. Chem. A* 6 (2018) 4590–4604.
- [35] H. Yi, D. Huang, L. Qin, G. Zeng, C. Lai, M. Cheng, S. Ye, B. Song, X. Ren, X. Guo, Selective prepared carbon nanomaterials for advanced photocatalytic application in environmental pollutant treatment and hydrogen production, *Appl. Catal. B: Environ.* 239 (2018) 408–424.
- [36] Z. Juanjuan, L. Ruiyi, L. Zaijun, L. Junkang, G. Zhiguo, W. Guangli, Synthesis of nitrogen-doped activated graphene aerogel/gold nanoparticles and its application for electrochemical detection of hydroquinone and o-dihydroxybenzene, *Nanoscale* 6 (2014) 5458–5466.
- [37] Q. Huang, F. Tao, L. Zou, T. Yuan, Z. Zou, H. Zhang, X. Zhang, H. Yang, One-step synthesis of Pt nanoparticles highly loaded on graphene aerogel as durable oxygen reduction electrocatalyst, *Electrochim. Acta* 152 (2015) 140–145.
- [38] L. Fernandez, V.I. Esteves, A. Cunha, R.J. Schneider, J.P. Tomé, Photodegradation of organic pollutants in water by immobilized porphyrins and phthalocyanines, *J. Porphyr. Phthalocya.* 20 (2016) 150–166.
- [39] W. Jiang, Y. Zhu, G. Zhu, Z. Zhang, X. Chen, W. Yao, Three-dimensional photocatalysts with a network structure, *J. Mater. Chem. A* 5 (2017) 5661–5679.
- [40] Y. Li, W. Cui, L. Liu, R. Zong, W. Yao, Y. Liang, Y. Zhu, Removal of Cr (VI) by 3D  $\text{TiO}_2$ -graphene hydrogel via adsorption enriched with photocatalytic reduction, *Appl. Catal. B: Environ.* 199 (2016) 412–423.
- [41] R. Zhang, W. Wan, L. Qiu, Y. Wang, Y. Zhou, Preparation of hydrophobic polyvinyl alcohol aerogel via the surface modification of boron nitride for environmental remediation, *Appl. Sur. Sci.* 419 (2017) 342–347.
- [42] C. Han, N. Zhang, Y.-J. Xu, Structural diversity of graphene materials and their multifarious roles in heterogeneous photocatalysis, *Nano Today* 11 (2016) 351–372.
- [43] L. Zhang, G. Shi, Preparation of highly conductive graphene hydrogels for fabricating supercapacitors with high rate capability, *J. Phys. Chem. C* 115 (2011) 17206–17212.
- [44] S. Stankovich, D.A. Dikin, R.D. Piner, K.A. Kohlhaas, A. Kleinhammes, Y. Jia, Y. Wu, S.T. Nguyen, R.S. Ruoff, Synthesis of graphene-based nanosheets via chemical reduction of exfoliated graphite oxide, *Carbon* 45 (2007) 1558–1565.
- [45] X. Xiao, T.E. Beechem, M.T. Brumbach, T.N. Lambert, D.J. Davis, J.R. Michael, C.M. Washburn, J. Wang, S.M. Brozik, D.R. Wheeler, Lithographically defined three-dimensional graphene structures, *ACS Nano* 6 (2012) 3573–3579.
- [46] L. Shi, K. Chen, R. Du, A. Bachmatiuk, M.H. Rümmler, K. Xie, Y. Huang, Y. Zhang, Z. Liu, Scalable seashell-based chemical vapor deposition growth of three-dimensional graphene foams for oil–water separation, *J. Am. Chem. Soc.* 138 (2016) 6360–6363.
- [47] C. Li, H. Bai, G. Shi, Conducting polymer nanomaterials: electrosynthesis and applications, *Chem. Soc. Rev.* 38 (2009) 2397–2409.
- [48] Z. Chen, W. Ren, L. Gao, B. Liu, S. Pei, H.-M. Cheng, Three-dimensional flexible and conductive interconnected graphene networks grown by chemical vapour deposition, *Nat. Mater.* 10 (2011) 424.
- [49] M. Nawaz, W. Miran, J. Jang, D.S. Lee, One-step hydrothermal synthesis of porous 3D reduced graphene oxide/ $\text{TiO}_2$  aerogel for carbamazepine photodegradation in aqueous solution, *Appl. Catal. B: Environ.* 203 (2017) 85–95.
- [50] J. Mao, J. Iocozzia, J. Huang, K. Meng, Y. Lai, Z. Lin, Graphene aerogels for efficient energy storage and conversion, *Synth. Lect. Energy Environ. Technol. Sci. Soc.* 11 (2018) 772–799.
- [51] H. Hu, Z. Zhao, Y. Gogotsi, J. Qiu, Compressible carbon nanotube–graphene hybrid aerogels with superhydrophobicity and superoleophilicity for oil sorption, *Environ. Sci. Technol. Lett.* 1 (2014) 214–220.
- [52] M.A. Worsley, P.J. Pauzauskie, T.Y. Olson, J. Biener, J.H. Satcher Jr, T.F. Baumann, Synthesis of graphene aerogel with high electrical conductivity, *J. Am. Chem. Soc.* 132 (2010) 14067–14069.
- [53] W. Chen, S. Li, C. Chen, L. Yan, Self-assembly and embedding of nanoparticles by in situ reduced graphene for preparation of a 3D Graphene/Nanoparticle aerogel, *Adv. Mat.* 23 (2011) 5679–5683.
- [54] L. Xiao, D. Wu, S. Han, Y. Huang, S. Li, M. He, F. Zhang, X. Feng, Self-assembled  $\text{Fe}_2\text{O}_3$ /graphene aerogel with high lithium storage performance, *ACS Appl. Mater. Interfaces* 5 (2013) 3764–3769.
- [55] J. Cao, L. Song, J. Tang, J. Xu, W. Wang, Z. Chen, Enhanced activity of Pd nanoparticles supported on Vulcan XC72R carbon pretreated via a modified Hummers method for formic acid electrooxidation, *Appl. Sur. Sci.* 274 (2013) 138–143.
- [56] A. Satti, P. Larpent, Y. Gun'ko, Improvement of mechanical properties of graphene oxide/poly (allylamine) composites by chemical crosslinking, *Carbon* 48 (2010) 3376–3381.
- [57] W. Chen, L. Yan, In situ self-assembly of mild chemical reduction graphene for three-dimensional architectures, *Nanoscale* 3 (2011) 3132–3137.
- [58] H. Bai, C. Li, G. Shi, Functional composite materials based on chemically converted graphene (*Adv. Mater.* 9/2011), *Adv. Mater.* 23 (2011) 1088–1088.
- [59] B. Das, B. Choudhury, A. Gomathi, A.K. Manna, S. Pati, C. Rao, Interaction of inorganic nanoparticles with graphene, *Chem. Phys. Chem.* 12 (2011) 937–943.
- [60] H. Vedala, D.C. Sorescu, G.P. Kotchey, A. Star, Chemical sensitivity of graphene edges decorated with metal nanoparticles, *Nano Lett.* 11 (2011) 2342–2347.
- [61] C. Ban, Z. Wu, D.T. Gillaspie, L. Chen, Y. Yan, J.L. Blackburn, A.C. Dillon, Nanostructured  $\text{Fe}_3\text{O}_4$ /swnt electrode: binder-free and high-rate li-ion anode, *Adv. Mat.* 22 (2010) E145–E149.
- [62] M.Y. Kim, J. Lee, Chitosan fibrous 3D networks prepared by freeze drying, *Carbohydr. Polym.* 84 (2011) 1329–1336.
- [63] L. Yang, Y. Liu, R. Zhang, W. Li, P. Li, X. Wang, Y. Zhou, Enhanced visible-light photocatalytic performance of a monolithic tungsten oxide/graphene oxide aerogel for nitric oxide oxidation, *Chin. J. Catal.* 39 (2018) 646–653.
- [64] Z.-S. Wu, S. Yang, Y. Sun, K. Parvez, X. Feng, K. Müllen, 3D nitrogen-doped graphene aerogel-supported  $\text{Fe}_3\text{O}_4$  nanoparticles as efficient electrocatalysts for the oxygen reduction reaction, *J. Am. Chem. Soc.* 134 (2012) 9082–9085.
- [65] T. Wu, M. Chen, L. Zhang, X. Xu, Y. Liu, J. Yan, W. Wang, J. Gao, Three-dimensional graphene-based aerogels prepared by a self-assembly process and its excellent catalytic and absorbing performance, *J. Mater. Chem. A* 1 (2013) 7612–7621.
- [66] P.W. Sutter, J.-I. Flege, E.A. Sutter, Epitaxial graphene on ruthenium, *Nat. Mater.* 7 (2008) 406.
- [67] C. Shan, H. Tang, T. Wong, L. He, S.T. Lee, Facile synthesis of a large quantity of graphene by chemical vapor deposition: an advanced catalyst carrier, *Adv. Mater.* 24 (2012) 2491–2495.
- [68] D. Wei, B. Wu, Y. Guo, G. Yu, Y. Liu, Controllable chemical vapor deposition growth of few layer graphene for electronic devices, *Accounts Chem. Res.* 46 (2012) 106–115.
- [69] F. Rafeian, M. Hosseini, M. Jonoobi, Q. Yu, Development of hydrophobic nanocellulose-based aerogel via chemical vapor deposition for oil separation for water treatment, *Cellulose* 25 (2018) 4695–4710.
- [70] M.A. Worsley, T.T. Pham, A. Yan, S.J. Shin, J.R. Lee, M. Bagge-Hansen, W. Mickelson, A. Zettl, Synthesis and characterization of highly crystalline graphene aerogels, *ACS Nano* 8 (2014) 11013–11022.
- [71] K.-x. Sheng, Y.-x. Xu, L. Chun, G.-q. Shi, High-performance self-assembled graphene hydrogels prepared by chemical reduction of graphene oxide, *New Carbon Mat.* 26 (2011) 9–15.
- [72] S. Pei, J. Zhao, J. Du, W. Ren, H.-M. Cheng, Direct reduction of graphene oxide films into highly conductive and flexible graphene films by hydrohalic acids, *Carbon* 48 (2010) 4466–4474.
- [73] I.K. Moon, J. Lee, R.S. Ruoff, H. Lee, Reduced graphene oxide by chemical graphitization, *Nat. Commun.* 1 (2010) 1–6.
- [74] S. Park, J. An, J.R. Potts, A. Velamakanni, S. Murali, R.S. Ruoff, Hydrazine-reduction of graphite-and graphene oxide, *Carbon* 49 (2011) 3019–3023.
- [75] X. Zhang, Z. Sui, B. Xu, S. Yue, Y. Luo, W. Zhan, B. Liu, Mechanically strong and highly conductive graphene aerogel and its use as electrodes for electrochemical power sources, *J. Mat. Chem.* 21 (2011) 6494–6497.
- [76] M.A. Worsley, S.O. Kucheyev, H.E. Mason, M.D. Merrill, B.P. Mayer, J. Lewicki, C.A. Valdez, M.E. Suss, M. Stadermann, P.J. Pauzauskie, Mechanically robust 3D graphene macroassembly with high surface area, *Chem. Commun.* 48 (2012) 8428–8430.
- [77] Z. Wang, X. Shen, M. Akbari Garakani, X. Lin, Y. Wu, X. Liu, X. Sun, J.-K. Kim, Graphene aerogel/epoxy composites with exceptional anisotropic structure and properties, *ACS Appl. Mater. Interfaces* 7 (2015) 5538–5549.
- [78] N. Zhang, M.-Q. Yang, S. Liu, Y. Sun, Y.-J. Xu, Waltzing with the versatile platform of graphene to synthesize composite photocatalysts, *Chem. Rev.* 115 (2015) 10307–10377.
- [79] Y. Lu, B. Ma, Y. Yang, E. Huang, Z. Ge, T. Zhang, S. Zhang, L. Li, N. Guan, Y. Ma, High activity of hot electrons from bulk 3D graphene materials for efficient photocatalytic hydrogen production, *Nano Res.* 10 (2017) 1662–1672.
- [80] J. Yang, D. Chen, Y. Zhu, Y. Zhang, Y. Zhu, 3D-3D porous  $\text{Bi}_2\text{WO}_6$ /graphene hydrogel composite with excellent synergistic effect of adsorption-enrichment and photocatalytic degradation, *Appl. Catal. B: Environ.* 205 (2017) 228–237.
- [81] A. Wold, Photocatalytic properties of titanium dioxide ( $\text{TiO}_2$ ), *Chem. Mat.* 5 (1993) 280–283.
- [82] L. Zhang, J. Li, Z. Chen, Y. Tang, Y. Yu, Preparation of Fenton reagent with  $\text{H}_2\text{O}_2$  generated by solar light-illuminated nano-Cu $2\text{O}$ /MWNTs composites, *Appl. Catal. A Gen.* 299 (2006) 292–297.
- [83] L. Zhao, X. Chen, X. Wang, Y. Zhang, W. Wei, Y. Sun, M. Antonietti, M.M. Titirici, One-step solvothermal synthesis of a carbon@ $\text{TiO}_2$  dyade structure effectively promoting visible-light photocatalysis, *Adv. Mater.* 22 (2010) 3317–3321.
- [84] L.-S. Zhang, K.-H. Wong, H.-Y. Yip, C. Hu, J.C. Yu, C.-Y. Chan, P.-K. Wong, Effective photocatalytic disinfection of *E. coli* K-12 using  $\text{AgBr}-\text{Ag}-\text{Bi}_2\text{WO}_6$  nanojunction system irradiated by visible light: the role of diffusing hydroxyl radicals, *Environ. Sci. Technol.* 44 (2010) 1392–1398.
- [85] K. He, Z. Zeng, A. Chen, G. Zeng, R. Xiao, P. Xu, Z. Huang, J. Shi, L. Hu, G. Chen, Advancement of Ag-graphene based nanocomposites: an overview of synthesis and its applications, *Small* 14 (2018) 1800871.
- [86] Y. Yang, Z. Zeng, C. Zhang, D. Huang, G. Zeng, R. Xiao, C. Lai, C. Zhou, H. Guo, W. Xue, Construction of iodine vacancy-rich  $\text{BiOI}/\text{Ag}@\text{AgI}$  Z-scheme heterojunction photocatalysts for visible-light-driven tetracycline degradation: transformation pathways and mechanism insight, *Chem. Eng. J.* 349 (2018) 808–821.
- [87] C. Zhou, C. Lai, C. Zhang, G. Zeng, D. Huang, M. Cheng, L. Hu, W. Xiong, M. Chen, J. Wang, Semiconductor/boron nitride composites: synthesis, properties, and

- photocatalysis applications, *Appl. Catal. B: Environ.* 238 (2018) 6–18.
- [88] C. Zhou, C. Lai, D. Huang, G. Zeng, C. Zhang, M. Cheng, L. Hu, J. Wan, W. Xiong, M. Wen, Highly porous carbon nitride by supramolecular preassembly of monomers for photocatalytic removal of sulfamethazine under visible light driven, *Appl. Catal. B: Environ.* 220 (2018) 202–210.
- [89] H. Wang, L. Zhang, Z. Chen, J. Hu, S. Li, Z. Wang, J. Liu, X. Wang, Semiconductor heterojunction photocatalysts: design, construction, and photocatalytic performances, *Chem. Soc. Rev.* 43 (2014) 5234–5244.
- [90] Q. Xiang, J. Yu, M. Jaroniec, Graphene-based semiconductor photocatalysts, *Chem. Soc. Rev.* 41 (2012) 782–796.
- [91] J.-J. Zhang, Y.-H. Wu, J.-Y. Mei, G.-P. Zheng, T.-T. Yan, X.-C. Zheng, P. Liu, X.-X. Guan, Synergetic adsorption and photocatalytic degradation of pollutants over 3D TiO<sub>2</sub>–graphene aerogel composites synthesized via a facile one-pot route, *Photochem. Photobiol. Sci.* 15 (2016) 1012–1019.
- [92] X. Yu, J. Shi, L. Feng, C. Li, L. Wang, A three-dimensional BiOBr/RGO heterostructural aerogel with enhanced and selective photocatalytic properties under visible light, *Appl. Sur. Sci.* 396 (2017) 1775–1782.
- [93] S. Song, W. Gao, X. Wang, X. Li, D. Liu, Y. Xing, H. Zhang, Microwave-assisted synthesis of BiOBr/graphene nanocomposites and their enhanced photocatalytic activity, *Dalton Trans.* 41 (2012) 10472–10476.
- [94] Z. Jiang, F. Yang, G. Yang, L. Kong, M.O. Jones, T. Xiao, P.P. Edwards, The hydrothermal synthesis of BiOBr flakes for visible-light-responsive photocatalytic degradation of methyl orange, *J. Photochem. Photobiol. A: Chem.* 212 (2010) 8–13.
- [95] Y. Yang, C. Zhang, C. Lai, G. Zeng, D. Huang, M. Cheng, J. Wang, F. Chen, C. Zhou, W. Xiong, BiOX (X = Cl, Br, I) photocatalytic nanomaterials: applications for fuels and environmental management, *Adv. Colloid. Interfac. Sci.* 254 (2018) 76–93.
- [96] X. Liu, J. Wang, Y. Dong, H. Li, Y. Xia, H. Wang, One-step synthesis of Bi<sub>2</sub>MoO<sub>6</sub>/reduced graphene oxide aerogel composite with enhanced adsorption and photocatalytic degradation performance for methylene blue, *Mat. Sci. Semicon. Proc.* 88 (2018) 214–223.
- [97] J.-J. Zhang, P. Qi, J. Li, X.-C. Zheng, P. Liu, X.-X. Guan, G.-P. Zheng, Three-dimensional Fe<sub>2</sub>O<sub>3</sub>–TiO<sub>2</sub>–graphene aerogel nanocomposites with enhanced adsorption and visible light-driven photocatalytic performance in the removal of RhB dyes, *J. Ind. Eng. Chem.* 61 (2018) 407–415.
- [98] Y. Yang, C. Zhang, D. Huang, G. Zeng, J. Huang, C. Lai, C. Zhou, W. Wang, H. Guo, W. Xue, Boron nitride quantum dots decorated ultrathin porous g-C<sub>3</sub>N<sub>4</sub>: intensified exciton dissociation and charge transfer for promoting visible-light-driven molecular oxygen activation, *Appl. Catal. B: Environ.* 245 (2019) 87–99.
- [99] W.-J. Ong, L.-L. Tan, S.-P. Chai, S.-T. Yong, Graphene oxide as a structure-directing agent for the two-dimensional interface engineering of sandwich-like graphene–gC<sub>3</sub>N<sub>4</sub> hybrid nanostructures with enhanced visible-light photo-reduction of CO<sub>2</sub> to methane, *Chem. Commun.* 51 (2015) 858–861.
- [100] Z. Tong, D. Yang, T. Xiao, Y. Tian, Z. Jiang, Biomimetic fabrication of g-C<sub>3</sub>N<sub>4</sub>/TiO<sub>2</sub> nanosheets with enhanced photocatalytic activity toward organic pollutant degradation, *Chem. Eng. J.* 260 (2015) 117–125.
- [101] X. Wang, S. Blechert, M. Antonietti, Polymeric graphitic carbon nitride for heterogeneous photocatalysis, *ACS Catal.* 2 (2012) 1596–1606.
- [102] L. Tang, C.-t. Jia, Y.-c. Xue, L. Li, A.-q. Wang, G. Xu, N. Liu, M.-h. Wu, Fabrication of compressible and recyclable macroscopic g-C<sub>3</sub>N<sub>4</sub>/GO aerogel hybrids for visible-light harvesting: a promising strategy for water remediation, *Appl. Catal. B: Environ.* 219 (2017) 241–248.
- [103] W. Wan, S. Yu, F. Dong, Q. Zhang, Y. Zhou, Efficient C<sub>3</sub>N<sub>4</sub>/graphene oxide macroscopic aerogel visible-light photocatalyst, *J. Mater. Chem. A* 4 (2016) 7823–7829.
- [104] H. He, L. Huang, Z. Zhong, S. Tan, Constructing three-dimensional porous graphene-carbon quantum dots/g-C<sub>3</sub>N<sub>4</sub> nanosheet aerogel metal-free photocatalyst with enhanced photocatalytic activity, *Appl. Sur. Sci.* 441 (2018) 285–294.
- [105] I.K. Moon, S. Yoon, K.Y. Chun, J. Oh, Highly elastic and conductive n-doped monolithic graphene aerogels for multifunctional applications, *Adv. Funct. Mater.* 25 (2015) 6976–6984.
- [106] S.-D. Jiang, G. Tang, Y.-F. Ma, Y. Hu, L. Song, Synthesis of nitrogen-doped graphene–ZnS quantum dots composites with highly efficient visible light photo-degradation, *Mater. Chem. Phys.* 151 (2015) 34–42.
- [107] Y. Liu, S. Wang, S. Xu, S. Cao, Evident improvement of nitrogen-doped graphene on visible light photocatalytic activity of N-TiO<sub>2</sub>/N-graphene nanocomposites, *Mater. Res. Bull.* 65 (2015) 27–35.
- [108] F. Meng, J. Li, S.K. Cushing, M. Zhi, N. Wu, Solar hydrogen generation by nanoscale p–n junction of p-type molybdenum disulfide/n-type nitrogen-doped reduced graphene oxide, *J. Am. Chem. Soc.* 135 (2013) 10286–10289.
- [109] Z. Tong, D. Yang, J. Shi, Y. Nan, Y. Sun, Z. Jiang, Three-dimensional porous aerogel constructed by g-C<sub>3</sub>N<sub>4</sub> and graphene oxide nanosheets with excellent visible-light photocatalytic performance, *ACS Appl. Mater. Interfaces* 7 (2015) 25693–25701.
- [110] S. Yan, Z. Li, Z. Zou, Photodegradation performance of g-C<sub>3</sub>N<sub>4</sub> fabricated by directly heating melamine, *Langmuir* 25 (2009) 10397–10401.
- [111] J. Mao, T. Peng, X. Zhang, K. Li, L. Ye, L. Zan, Effect of graphitic carbon nitride microstructures on the activity and selectivity of photocatalytic CO<sub>2</sub> reduction under visible light, *Catal. Sci. Technol.* 3 (2013) 1253–1260.
- [112] W. Zhao, Y. Guo, S. Wang, H. He, C. Sun, S. Yang, A novel ternary plasmonic photocatalyst: ultrathin g-C<sub>3</sub>N<sub>4</sub> nanosheet hybridized by Ag/AgVO<sub>3</sub> nanoribbons with enhanced visible-light photocatalytic performance, *Appl. Catal. B: Environ.* 165 (2015) 335–343.
- [113] Y.-H. Zhang, Y. Zhao, N. Li, Y.-C. Peng, E. Giannoulatou, R.-H. Jin, H.-P. Yan, H. Wu, J.-H. Liu, N. Liu, Interferon-induced transmembrane protein-3 genetic variant rs12252-C is associated with severe influenza in Chinese individuals, *Nat. Commun.* 4 (2013) 1–6.
- [114] D. Ma, J. Wu, M. Gao, Y. Xin, T. Ma, Y. Sun, Fabrication of Z-scheme g-C<sub>3</sub>N<sub>4</sub>/RGO/Bi<sub>2</sub>WO<sub>6</sub> photocatalyst with enhanced visible-light photocatalytic activity, *Chem. Eng. J.* 290 (2016) 136–146.
- [115] Q. Li, N. Zhang, Y. Yang, G. Wang, D.H. Ng, High efficiency photocatalyst for pollutant degradation with MoS<sub>2</sub>/C<sub>3</sub>N<sub>4</sub> heterostructures, *Langmuir* 30 (2014) 8965–8972.
- [116] X. Yu, P. Wu, C. Qi, J. Shi, L. Feng, C. Li, L. Wang, Ternary-component reduced graphene oxide aerogel constructed by g-C<sub>3</sub>N<sub>4</sub>/BiOBr heterojunction and graphene oxide with enhanced photocatalytic performance, *J. Alloys Compd.* 729 (2017) 162–170.
- [117] J.-J. Zhang, S.-S. Fang, J.-Y. Mei, G.-P. Zheng, X.-C. Zheng, X.-X. Guan, High-efficiency removal of rhodamine B dye in water using g-C<sub>3</sub>N<sub>4</sub> and TiO<sub>2</sub> co-hybridized 3D graphene aerogel composites, *Sep. Purif. Technol.* 194 (2018) 96–103.
- [118] X. Yan, R. Xu, J. Guo, X. Cai, D. Chen, L. Huang, Y. Xiong, S. Tan, Enhanced photocatalytic activity of Cu<sub>2</sub>O/g-C<sub>3</sub>N<sub>4</sub> heterojunction coupled with reduced graphene oxide three-dimensional aerogel photocatalysis, *Mater. Res. Bull.* 96 (2017) 18–27.
- [119] Y. Ma, J. Wang, S. Xu, S. Feng, J. Wang, Ag<sub>2</sub>O/sodium alginate-reduced graphene oxide aerogel beads for efficient visible light driven photocatalysis, *Appl. Sur. Sci.* 430 (2018) 155–164.
- [120] X. Xu, F. Ming, J. Hong, Y. Xie, Z. Wang, Three-dimensional porous aerogel constructed by Bi<sub>2</sub>WO<sub>6</sub> nanosheets and graphene with excellent visible-light photocatalytic performance, *Mater. Lett.* 179 (2016) 52–56.
- [121] W. Liu, J. Cai, Z. Li, Self-assembly of semiconductor nanoparticles/reduced graphene oxide (RGO) composite aerogels for enhanced photocatalytic performance and facile recycling in aqueous photocatalysis, *ACS Sustain. Chem. Eng.* 3 (2015) 277–282.
- [122] J. Choi, D.A. Reddy, M.J. Islam, R. Ma, T.K. Kim, Self-assembly of CeO<sub>2</sub> nanostructures/reduced graphene oxide composite aerogels for efficient photocatalytic degradation of organic pollutants in water, *J. Alloys Compd.* 688 (2016) 527–536.
- [123] X. Li, S. Yang, J. Sun, P. He, X. Xu, G. Ding, Tungsten oxide nanowire-reduced graphene oxide aerogel for high-efficiency visible light photocatalysis, *Carbon* 78 (2014) 38–48.
- [124] F. Chen, S. Li, Q. Chen, X. Zheng, P. Liu, S. Fang, 3D graphene aerogels-supported Ag and Ag@Ag<sub>3</sub>PO<sub>4</sub> heterostructure for the efficient adsorption-photocatalysis capture of different dye pollutants in water, *Mater. Res. Bull.* 105 (2018) 334–341.
- [125] M. Cheng, Y. Liu, D. Huang, C. Lai, G. Zeng, J. Huang, Z. Liu, C. Zhang, C. Zhou, L. Qin, Prussian blue analogue derived magnetic Cu-Fe oxide as a recyclable photo-Fenton catalyst for the efficient removal of sulfamethazine at near neutral pH values, *Chem. Eng. J.* 362 (2019) 865–876.
- [126] Y. Li, H. Xu, S. Ouyang, J. Ye, Metal–organic frameworks for photocatalysis, *J. Chem. Soc. Faraday Trans.* 18 (2016) 7563–7572.
- [127] J. Gascon, F. Kapteijn, Metal-Organic Framework Membranes—High Potential, Bright Future? *Angew. Chem. Int. Ed. English* 49 (2010) 1530–1532.
- [128] J. Mao, M. Ge, J. Huang, Y. Lai, C. Lin, K. Zhang, K. Meng, Y. Tang, Constructing multifunctional MOF@rGO hydro-aerogels by the self-assembly process for customized water remediation, *J. Mater. Chem. A* 5 (2017) 11873–11881.
- [129] C. Fan, Q. Liu, T. Ma, J. Shen, Y. Yang, H. Tang, Y. Wang, J. Yang, Fabrication of 3D CeVO<sub>4</sub>/graphene aerogels with efficient visible-light photocatalytic activity, *Ceram. Int.* 42 (2016) 10487–10492.
- [130] Y. Li, J. Yang, S. Zheng, W. Zeng, N. Zhao, M. Shen, One-pot synthesis of 3D TiO<sub>2</sub>-reduced graphene oxide aerogels with superior adsorption capacity and enhanced visible-light photocatalytic performance, *Ceram. Int.* 42 (2016) 19091–19096.
- [131] W. Liu, J. Cai, Z. Ding, Z. Li, TiO<sub>2</sub>/RGO composite aerogels with controllable and continuously tunable surface wettability for varied aqueous photocatalysis, *Appl. Catal. B: Environ.* 174 (2015) 421–426.
- [132] B. Qiu, M. Xing, J. Zhang, Mesoporous TiO<sub>2</sub> nanocrystals grown in situ on graphene aerogels for high photocatalysis and lithium-ion batteries, *J. Am. Chem. Soc.* 136 (2014) 5852–5855.
- [133] Z. Chen, J. Ma, K. Yang, S. Feng, W. Tan, Y. Tao, H. Mao, Y. Kong, Preparation of S-doped TiO<sub>2</sub>-three dimensional graphene aerogels as a highly efficient photocatalyst, *Synthetic Met.* 231 (2017) 51–57.
- [134] Y. Li, H. Yuan, A. Von Dem Bussche, M. Creighton, R.H. Hurt, A.B. Kane, H. Gao, Graphene microspheres enter cells through spontaneous membrane penetration at edge asperities and corner sites, *P. Natl. Acad. Sci.* 110 (2013) 12295–12300.
- [135] S. Gurunathan, J.-H. Kim, Synthesis, toxicity, biocompatibility, and biomedical applications of graphene and graphene-related materials, *Int. J. Nanomed. Nanosurg.* 11 (2016) 1927.
- [136] G. Wang, F. Qian, C.W. Saltikov, Y. Jiao, Y. Li, Microbial reduction of graphene oxide by *Shewanella*, *Nano Res.* 4 (2011) 563–570.
- [137] M.C. Duch, G.S. Buderger, Y.T. Liang, S. Soberanes, D. Urich, S.E. Chiarella, L.A. Campochiaro, A. Gonzalez, N.S. Chandel, M.C. Hersam, Minimizing oxidation and stable nanoscale dispersion improves the biocompatibility of graphene in the lung, *Nano Lett.* 11 (2011) 5201–5207.
- [138] J.-H. Liu, S.-T. Yang, H. Wang, Y. Chang, A. Cao, Y. Liu, Effect of size and dose on the biodistribution of graphene oxide in mice, *Nanomedicine* 7 (2012) 1801–1812.
- [139] X. Wang, R. Podila, J.H. Shannahan, A.M. Rao, J.M. Brown, Intravenously delivered graphene nanosheets and multiwalled carbon nanotubes induce site-specific Th2 inflammatory responses via the IL-33/ST2 axis, *Int. J. Nanomed. Nanosurg.* 8 (2013) 1733.